Chemistry of Metals and Alloys

Chem. Met. Alloys 6 (2013) 144-149
Ivan Franko National University of Lviv
www.chemetal-journal.org

Correlation between the milling time and phase-structural state of ZrCrNi and $ZrMn_2$ Laves phase alloys

Yurii BASARABA[1]*, Taras ZASADNYY[2]

[1] *Department of General and Applied Physics, Ivano-Frankivsk National Technical University of Oil and Gas, Karpatska St. 15, 76019 Ivano-Frankivsk, Ukraine*
[2] *Department of Hydrogen Technologies and Hydride Materials Science, Karpenko Physico-Mechanical Institute of the NAS of Ukraine, Naukova St. 5, 79601 Lviv, Ukraine*
* *Corresponding author. Tel.: +038-097-4984325; e-mail: yubasaraba@ukr.net*

Received September 21, 2013; accepted December 25, 2013; available on-line August 30, 2014

The phase content of ZrCrNi and $ZrMn_2$ alloys with initial hexagonal $MgZn_2$ (C14) type of Laves phase structure after reactive milling in hydrogen was investigated by X-ray powder diffraction and energy-dispersive X-ray spectroscopy. Depending on the milling time, the structure of the ZrCrNi alloy, which now contains significant amounts of Fe, changes from $MgZn_2$ type to $MgCu_2$ and Th_6Mn_{23} type structure after heat treatment.

Laves phases / Hydrogen / High-energy ball milling / X-ray powder diffraction / Crystal structure

Introduction

Laves phases with AB_2 compositions are a common type of topologically close-packed structure [1,2]. Laves phases are of particular interest in modern metallurgy research [3], hydrogen storage applications [4], and production of secondary batteries [5] because of their unusual physical and chemical properties. Furthermore, Laves phases are capable of dissolving considerable amounts of alloying additions. Among the alloys for negative electrodes of nickel-metal hydride batteries, Zr-based Laves phase alloys have attracted attention due to their high electrochemical capacity and cycle life. They are based on the stoichiometric compounds ZrV_2, $ZrCr_2$ and $ZrMn_2$. $ZrCr_2$ crystallizing in the hexagonal C14 type of structure is one of the interesting candidates, but it is not used as hydrogen storage material for negative electrodes of nickel-metal hydride batteries [6], due to the excessive stability of its hydride (dissociation equilibrium pressure of 5 kPa at 353 K [7]). However, the replacement of chromium by other elements (*i.e.* nickel, iron) can modify the crystal structure, the dissociation pressure of hydrogen and discharge capacity. Another way to modify the crystal structure is the well known ball milling process [8]. The mechanical ball milling process in hydrogen and argon atmosphere, in the presence of a fluid, was introduced to produce amorphous materials. Recently, this process was adopted to synthesize intermetallics and other inorganic compounds [8]. When the ball milling technique is used for such syntheses, the powders produced show unusual characteristics, and it is possible to obtain nanocrystalline structures [9], amorphous materials [10] and alloys with extended solubility. Heating in vacuum is carried out to crystallize the amorphous material. Moreover, nanocrystalline alloys have attracted interest because their hydriding properties are different from those of the conventional crystalline alloys.

This work presents a study on phase-structural aspects of high-energy ball-milled ZrCrNi and $ZrMn_2$ alloys before and after heating in vacuum. The expedience and perspectives of high-energy milling of Laves phase alloys with the aim to modify their structure are discussed.

Experimental

The ZrCrNi and $ZrMn_2$ alloys were prepared by arc melting with a non-consumable (W) electrode under a reduced pressure argon atmosphere on a water-cooled copper hearth. The ingots were re-melted three times to ensure homogeneity throughout the ingot. Raw materials were Zr, Cr, Ni, Mn of at least 99.7% purity. The weight loss of each alloy during melting was less than 1%, and, the compositions of the alloys can therefore be regarded as the same as the nominal ones. The as-cast alloy was pulverized by hydrating under 50 atm.

The pulverized alloys were put into a CrNi steel bowl together with stainless steel balls (10 mm in diameter). Ball milling was carried out using a planetary ball mill at a speed of 600 rpm. The bowl was filled with hydrogen to a pressure of 7 atm. The ball-to-powder weight ratio was 80:1. For crystallization of the amorphous materials after milling, the powdered alloys were heated in vacuum to 950ºC.

X-ray diffraction patterns were recorded on a DRON-3 diffractometer using Fe-K_α and Cu-K_α radiation ($10^o \le 2\theta \le 140^o$ range, 0.05º scan step, 18 s exposures at each point for the phase analysis and refinement of the structure parameters). The structure refinement was performed using the full-profile Rietveld method included in the FullProf Suite and PowderCell software packages.

Energy-dispersive X-ray spectroscopy was performed with a scanning electron microscope EVO 40XVP with an energy dispersion X-ray spectrometer INCA Energy 350 (Carl Zeiss, Germany and Oxford Instruments, UK).

Results and discussion

$ZrMn_2$ alloy

The X-ray phase analysis of the $ZrMn_2$ alloy indicates that the major phase of this alloy has hexagonal $MgZn_2$ (C14) type Laves phase structure (see Fig. 1*a*, Table 1). Before milling, the samples were hydrogenated in an autoclave under a hydrogen pressure of 50 atm. The diffractograms of the hydrogenated samples show C14 hexagonal $MgZn_2$ type structure, with increased lattice parameters equal to a = 0.5444 nm and c = 0.8850 nm. The hydrides were loaded into the bowl of a planetary ball mill; the bowl was evacuated and filled with hydrogen to a pressure of 7 atm. Milling was carried out for 1, 8, 16, and 24 h. As a result of the milling, the initial phase was decomposed. Zirconium hydride and manganese are the main phases formed after milling (Fig. 1*b*). An increase of the milling time led to an increase of the intensity of the manganese peak (330).

After milling, the samples were heated in vacuum to 950ºC. After milling for 1 h the alloy powder crystallized in the initial hexagonal $MgZn_2$ (C14) type Laves phase structure, but with decreased lattice parameters as compared with the original phase (Table 1). An increase of the milling time to 8 h or more caused the formation of a Th_6Mn_{23} type structure and release of manganese (Fig. 1*c*). It is known that such a compound does not exist in the Zr–Mn system [11]. However, it exists in the Zr–Fe system [12]. Energy-dispersive X-ray analysis showed the presence of iron (39.54 wt.% after 16 h and 45.88 wt.% after 24 h) in the samples after milling. It was found that the lattice parameter of the compound with Th_6Mn_{23}-type structure decreases with increasing milling time (Table 1). This can be explained by progressive replacement of manganese by iron, which enters the bowl as a result of abrasion of ball material.

It should be noted that Laves phase on the base of $ZrMn_2$ interacts well with hydrogen and forms hydrides. $ZrMn_2$ has a hydrogen capacity of 1.2 H/*M* and is the basis for the development of materials for hydrogen storage and negative electrodes of nickel-metal hydride batteries. The compound itself is not used because of the high stability of its hydrides. The replacement of manganese by other transition metals, such as iron [13], can reduce the stability of the hydrides. Samples obtained after milling for 1 h may form less stable hydrides.

Table 1 Crystallographic data and experimental details for the $ZrMn_2$ alloy (initial composition: Zr – 45.67 wt.%, Mn – 54.33 wt.%) after milling and heating in vacuum to 950ºC.

Parameter	Initial	Milling time (h)			
		1	8	16	24
Structure type	$MgZn_2$	$MgZn_2$	Th_6Mn_{23}[a]	Th_6Mn_{23}[a]	Th_6Mn_{23}[a]
Space group	*P*6$_3$/*mmc*	*P*6$_3$/*mmc*	*Fm*-3*m*	*Fm*-3*m*	*Fm*-3*m*
a (Å)	5.025(4)	4.995(3)	11.747(8)	11.729(3)	11.726(5)
c (Å)	8.256(5)	8.185(7)	–	–	–
Cell volume (Å^3)	180.57(6)	176.68(8)	1621.32(8)	1613.67(5)	1612.52(6)
Pearson symbol	*hP*12	*hP*12	*cF*116	*cF*116	*cF*116
Calculated density (g/cm^3)	7.395	7.560	7.661	7.678	7.696
Radiation and wavelength (Å)	Fe 1.93728	Fe 1.93728	Fe 1.93728	Fe 1.93728	Fe 1.93728
Mode of refinement	Full profile	Full profile	Full profile	Full profile	Full profile
Profile parameters *U*	-0.068654	0.159438	-0.004107	0.057591	-0.180593
V	0.384405	0.046597	0.389843	0.304974	0.642024
W	-0.110942	0.012193	-0.104158	-0.104158	-0.166007
R_p (%)	2.52	2.27	2.26	1.99	2.77
R_{wp} (%)	3.26	2.98	3.28	2.72	3.71
R_{exp} (%)	1.97	2.00	2.26	1.47	0.78
Scale factor	1.178	1.030	0.657	0.993	1.148

[a] A small amount of manganese precipitation was detected.

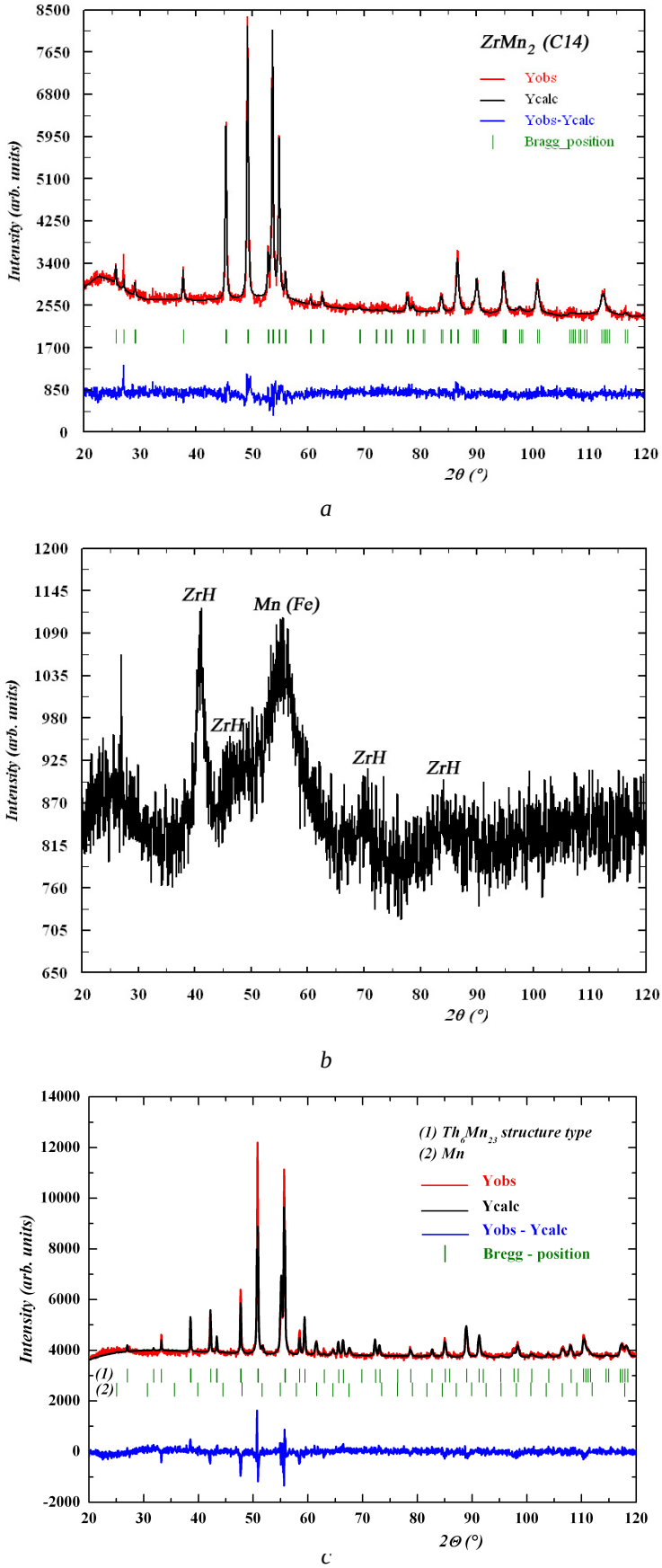

Fig. 1 Experimental X-ray powder patterns of $ZrMn_2$ alloys: *a* – initial; *b* – after milling in hydrogen for 16 h; *c* – after heat treatment in vacuum.

ZrCrNi alloy

The X-ray phase analysis of the ZrCrNi alloy indicates that the major phase of this alloy has hexagonal $MgZn_2$ (C14) type Laves phase structure (Fig. 2*a*, Table 2) [14,15]. A small amount of Zr–Ni compounds was also observed. After milling in hydrogen, amorphous products were formed (Fig. 2*b*). Heating in vacuum to 950ºC led to the formation of the cubic $MgCu_2$ (C15) type of Laves phase structure (Fig. 2*c*).

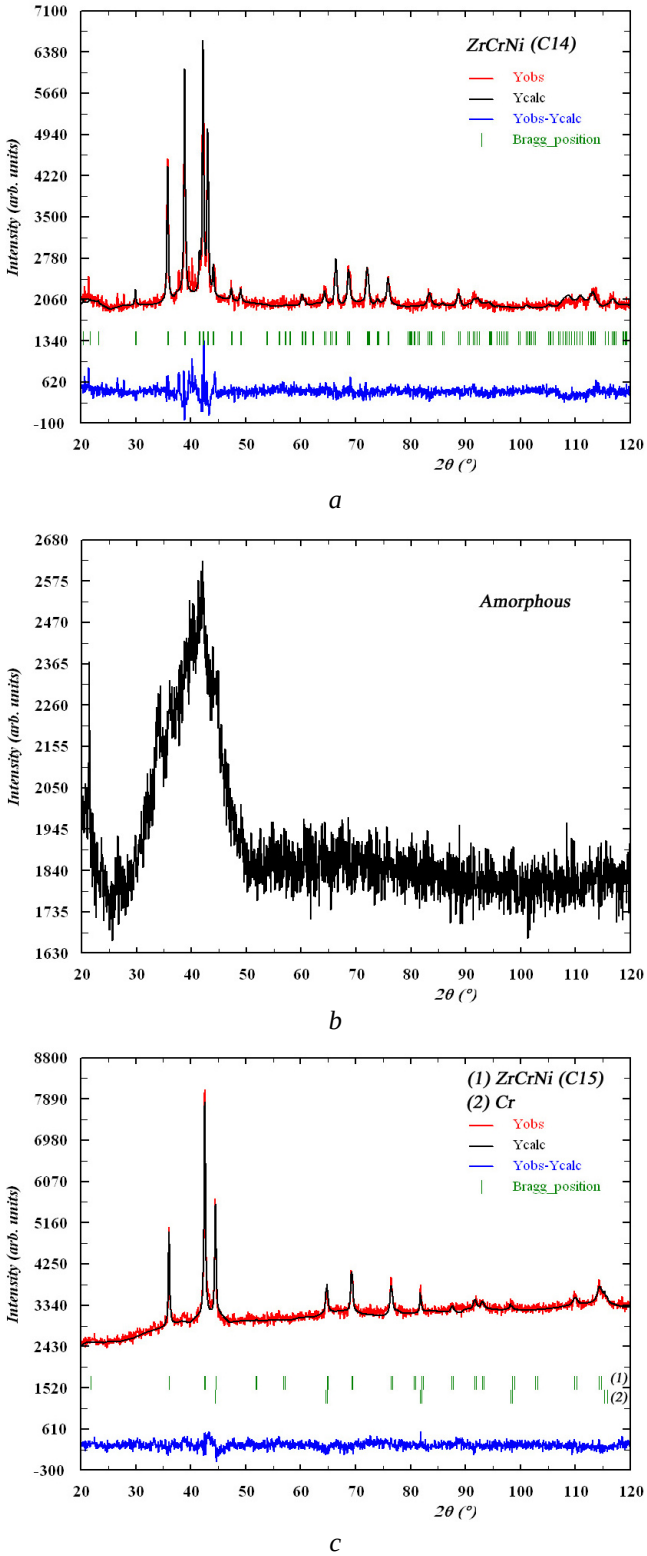

Fig. 2 Experimental X-ray powder patterns of the ZrCrNi alloy: *a* – initial; *b* – after milling in hydrogen for 1 h; *c* – after heat treatment in vacuum.

This occurred when the milling time ranged from 10 min to 4 h. For milling times between 8 h and 24 h, after heat treatment in vacuum the material crystallized in the cubic Th_6Mn_{23} structure type (Table 2). Thus, depending on the milling time, the structure of the alloy changes from $MgZn_2$ type to $MgCu_2$ or Th_6Mn_{23} type during the heat treatment. After milling for 8 h, the two phases C15 and $Zr_6(Ni,Cr,Fe)_{23}$ coexisted (Table 2). The reason for the change of structure is the presence of iron, which enters the sample as a result of abrasion of the balls used for milling (Table 3). Moreover, the amount of iron in the sample is proportional to the milling time. Tungsten and manganese are the alloying elements of the stainless steel from which the balls and bowl are made.

High-energy milling of these alloys under these conditions in hydrogen atmosphere should be performed up to 4 h, if the alloys should be used for hydrogen storage. For investigation in the field of stainless steel-zirconium alloys, milling can be carried out for a longer time [16,17].

Conclusions

On the basis of the obtained data, it could be concluded that the main phase of ZrCrNi and $ZrMn_2$ alloys after high-energy milling and heat treatment in vacuum is changed from the hexagonal $MgZn_2$ (C14) type of Laves phase into the Th_6Mn_{23} type of structure when the time of grinding is 8-24 h. This is due to the fact that iron enters the sample as a result of abrasion of the balls. After milling for 1-4 h the ZrCrNi alloy crystallizes in a cubic $MgCu_2$ type structure and $ZrMn_2$ crystallizes in the initial hexagonal $MgZn_2$ (C14) type of Laves phase with reduced lattice parameters.

Table 2 Crystallographic data and experimental details for the ZrCrNi alloy (initial composition: Zr – 46.54 wt.%, Cr – 24.40 wt.%, Ni – 29.06 wt.%) after milling and heating in vacuum to 950ºC.

Parameter	Initial	Milling time (h)				
		1	8		16	24
Type of structure	$MgZn_2$	$MgCu_2$	$MgCu_2$	Th_6Mn_{23}	Th_6Mn_{23}	Th_6Mn_{23}
Phase content (wt.%)[a]	100	78.6	28.8	46.5	68	49.5
Space group	*P*6$_3$/*mmc*	*Fd*-3*m*	*Fd*-3*m*	*Fm*-3*m*	*Fm*-3*m*	*Fm*-3*m*
a (Å)	5.011(1)	7.039(1)	6.974(3)	11.665(2)	11.646(3)	11.631(8)
c (Å)	8.205(6)	–	–	–	–	–
Cell volume (Å^3)	178.43(6)	348.78(3)	339.05(4)	1587.36(3)	1579.66(5)	1573.77(9)
Pearson symbol	*hP*12	*cF*24	*cF* 24	*cF*116	*cF*116	*cF*116
Calculated density (g/cm^3)	7.286	7.423	7.649	8.189	7.845	7.858
Radiation and wavelength (Å)	Cu 1.54059	Cu 1.54059	Cu 1.54059	Cu 1.54059	Cu 1.54059	Cu 1.54059
Mode of refinement	Full profile	Full profile	Full profile	Full profile	Full profile	Full profile
Profile parameters *U*	0.500000	0.41967	0.02935	-0.02072	0.09087	0.89985
V	0.000000	0.04967	0.15072	0.19684	0.01223	-0.83974
W	0.100829	0.06314	0.05407	-0.02168	0.04331	0.32250
R_p (%)	2.88	2.31	5.40	1.86	1.55	1.67
R_{wp} (%)	4.41	3.13	7.46	2.40	1.98	2.15
R_{exp} (%)	0.59	0.66	1.15	0.48	0.65	0.59
Scale factor	1.496	0.57	0.329	0.531	0.574	0.350

[a] The rest is b.c.c. chromium.

Table 3 Elemental composition of the ZrCrNi alloy after milling.

Element	Milling time (h)							
	1		8		16		24	
	wt.%	at.%	wt.%	at.%	wt.%	at.%	wt.%	at.%
Cr	25.84	32.24	22.92	27.43	19.84	23.12	17.99	20.54
Fe	10.19	11.84	29.52	32.89	44.22	47.97	53.30	56.65
Ni	27.70	30.61	20.25	21.46	14.78	15.25	11.60	11.73
Zr	34.91	24.83	26.14	17.83	19.97	13.26	15.47	10.07
W	1.36	0.48	1.17	0.40	1.19	0.39	1.00	0.32
Mn	–	–	–	–	–	–	0.64	0.69

References

[1] F. Stein, M. Palm, G. Sauthoff, *Intermetallics* 12 (2004) 713-720.

[2] F. Stein, M. Palm, G. Sauthoff, *Intermetallics* 13 (2005) 1056-1074.

[3] N. Das, P. Sengupta, S. Roychowdhury, G. Sharma, P.S. Gawde, A. Arya, V. Kain, U.D. Kulkarni, J.K. Chakravartty, G.K. Dey, *J. Nucl. Mater*. 420 (2012) 559-574.

[4] H. Li, X. Wang, Zh. Dong, L. Xu, Ch. Chen, *J. Alloys Compd.* 502 (2010) 503-507.

[5] K. Young, T. Ouchi, J. Koch, M.A. Fetcenko, *J. Alloys Compd.* 510 (2012) 97-106.

[6] F.C. Ruiz, H.A. Peretti, A. Visintin, W.E. Triaca, *Int. J. Hydrogen Energy* 36 (2011) 901-906.

[7] A. Visintin, H.A. Peretti, C.A. Tori, W.E. Triaca, *Int. J. Hydrogen Energy* 26 (2001) 683-689.

[8] D. Guérard *Rev. Adv. Mater. Sci.* 18 (2008) 225-230.

[9] J. Ankur, A. Shivani, I.P. Jain, *J. Alloys Compd.* 480 (2009) 325-328.

[10] Ch.B. Jung, K.S. Lee, *J. Alloys Compd.* 274 (1998) 254-259.

[11] M.E. Schlesinger, *J. Phase Equilib.* 20 (1999) 79-83.

[12] J.E. Larson, J.K. Cook, R.J. Wermer, G.D. Tuggle, *J. Alloys Compd.* 330-332 (2002) 897-901.

[13] H. Okamoto, *J. Phase Equilib. Diffus.* 27 (2006) 543-544.

[14] J.-M. Joubert, M. Latroche, A. Percheron-Guégan, I. Ansara, *J. Phase Equilib*. 16 (1995) 485-492.

[15] Sh.-J. Luo, Ch.-H. Wang, S.-W. Chen, *Metall. Mater. Trans. A* 33 (2002) 995-1002.

[16] D.P. Abraham, J.W. Richardson, S.M. McDeavitt, *Mater. Sci. Eng., A* 239-240 (1997) 658-664.

[17] D.P. Abraham, N.L. Dietz, *Mater. Sci. Eng., A* 329-331 (2002) 610-615.